Aquat Sci (2017) 79:231–248
DOI 10.1007/s00027-016-0493-0

Aquatic Sciences

RESEARCH ARTICLE

CDOM and the underwater light climate in two shallow North Patagonian lakes: evaluating the effects on nano and microphytoplankton community structure

Marina Gerea[1,4] · Gonzalo L. Pérez[1,4] · Fernando Unrein[2,4] · Carolina Soto Cárdenas[1,4] · Donald Morris[3] · Claudia Queimaliños[1,4]

Received: 27 March 2015 / Accepted: 6 June 2016 / Published online: 13 June 2016

Abstract We performed an annual synchronous sampling in two oligotrophic shallow lakes to assess the influence of chromophoric dissolved organic matter (CDOM) on the underwater light climate, and its potential effects on the nano and microphytoplankton community structure. Lake Escondido showed higher CDOM concentration and light attenuation with a spectral composition of underwater light shifted towards green–yellow light, while Lake Morenito presented clearer waters and a dominance of green light. Temporal dynamics of CDOM absorption at 440 nm were consistently explained by differences in cumulative precipitation. Mixotrophic cryptophytes and chrysophytes dominated the phytoplankton of both lakes, although the prevalence of each algal group was different between lakes. The dominance of these groups was largely explained by differences in spectral composition of underwater light, estimated as the ratio between Kd(RED) and Kd(GREEN) [Kd(R)/Kd(G) ratio]. Cryptophytes prevailed in Lake Morenito and their biomass showed a positive strong relationship with Kd(R)/Kd(G) ratio. Chrysophyte biomass was comparatively more important in Lake Escondido showing an opposite relationship with the Kd(R)/Kd(G) ratio. These results underscore that higher relative green light availability allowed the dominance of cryptophytes, while changes in light spectral composition driven by CDOM allowed coexistence. We suggest that nano and microphytoplankton community structure in these lakes could be driven by changes in spectral composition of underwater light shaped by differences in CDOM, ultimately determined by precipitation/hydrological patterns.

Keywords Spectral composition of underwater light · Light climate · Nanophytoplankton · Microphytoplankton · Community structure

Introduction

Dissolved organic matter (DOM) is a critical component of aquatic systems, playing an important role in ecosystem function and structure. In freshwater ecosystems, sources of DOM are often dominated by allochthonous inputs from the surrounding watershed supplemented by autochthonous DOM generated by in-lake processes (e.g., Huang and Chen 2009; Mladenov et al. 2011; Hiriart-Baer 2013). Particularly, changes in rainfall patterns strongly influence DOM delivery to aquatic ecosystems. Consequently, climate change affects DOM inputs in lakes because large decreases in DOM might occur as a result of reduced runoff during periods of drought (Leavitt et al. 1997; Schindler et al. 1997; Pienitz and Vincent 2000). On the

Electronic supplementary material The online version of this article (doi:10.1007/s00027-016-0493-0) contains supplementary material, which is available to authorized users.

✉ Marina Gerea
geream@comahue-conicet.gob.ar

[1] Laboratorio de Fotobiología, INIBIOMA (Instituto Investigaciones en Biodiversidad y Medio Ambiente), Universidad Nacional del Comahue-CONICET, Quintral 1250, R8400FRD Bariloche, Argentina

[2] Laboratorio de Ecología y Fotobiología Acuática, IIB-INTECH (Instituto de Investigaciones Biotecnológicas-Instituto Tecnológico de Chascomús), UNSAM-CONICET, Av. Intendente Marino km 8,200, B7130IWA Chascomús, Argentina

[3] Department of Earth and Environmental Sciences, Lehigh University, Bethlehem, PA 18015-3188, USA

[4] Consejo Nacional de Investigación Científica y Técnica (CONICET), Buenos Aires, Argentina

other hand, counteractive effects could be expected with the increment of precipitation favoring runoff (Pace and Cole 2002; Hongve et al. 2004; Zepp et al. 2011). In addition, the chromophoric DOM (CDOM) absorbs solar radiation causing differential effects upon aquatic primary producers, protecting cells from harmful ultraviolet radiation (UVR) (Walsh et al. 2003; Häder et al. 2007) and decreasing light availability for photosynthesis (Jones 1992; Carpenter et al. 1998; Karlsson et al. 2009).

Light absorption by CDOM has been shown to be the major factor attenuating solar radiation in oligotrophic lakes (Bukaveckas and Robbins-Forbes 2000). In these lakes, empirical models have been developed to estimate attenuation of PAR and UVR from either DOC concentration or from absorption coefficients of CDOM (Scully and Lean 1994; Morris et al. 1995; Bukaveckas and Robbins-Forbes 2000). In high-latitude lakes, it has been shown that changes in CDOM associated with minor increases of DOC concentration (0.4 mg L^{-1}) are likely to cause drastic changes in water transparency, eliciting a significant decrease in the depth of the euphotic layer (Vincent et al. 1998). CDOM is not only important in regulating transparency and consequently the amount of solar energy in the water column; it can also determine the spectral composition of underwater irradiance. In clear water lakes, sunlight in the green part of the spectrum penetrates deepest, whereas in moderately stained waters green and red light penetrations are equal. Particularly, in very brown waters absorption by CDOM exceeds the absorption by water, and red light penetrates deepest (Kirk 2011). Framed in either ecological niche theory (Gause 1934) or chromatic adaptation theory (Engelmann 1883), several works have analyzed the importance of irradiance spectral composition in phytoplankton diversity and community composition. According to Stomp et al. (2007), plankton ecologists have long recognized that a rich variety of photosynthetic pigments allow phytoplankton species to utilize the different wavelengths (Falkowski et al. 2004; Kirk 2011), although competition theory has largely ignored the light spectrum as an important axis of niche differentiation. These pigment divergences allow a more efficient utilization of the available light energy, and contribute to the biodiversity of phototrophic microorganisms in aquatic environments (Stomp et al. 2004). For instance, red picocyanobacteria use the pigment phycoerythrin (PE) for harvesting prevailing green wavelengths, whereas the pigment phycocyanin (PC) present in the green picocyanobacteria harvests the light in red dominated underwater light climates (Vörös et al. 1998; Stomp et al. 2004, 2007). Previous investigations have mainly focused on the competition and niche differentiation of picocyanobacteria (e.g., Wood 1985; Pick 1991; Vörös et al. 1998; Wood et al. 1998; Palenik 2001; Stomp et al. 2004, 2007; Callieri 2007), while other phytoplankton groups remain poorly characterized. Indeed, the phycobilins are present in the cryptophytes as well, also conferring to these algae the ability to harvest sunlight that would not otherwise be used by other algal groups (Dinshaw 2012). Some studies have also demonstrated that the spectral composition of underwater light could be a significant determinant of community composition of other phytoplankton groups (Takahashi et al. 1989; Bidigare et al. 1990; Hickman et al. 2009, 2010; Lawrenz et al. 2010).

The Northwestern Patagonian region (37–41°S, ~71°W, Argentina), shows a cold-temperate climate, and is characterized by the presence of numerous deep ultra-oligotrophic lakes of glacial origin. These lakes are situated in areas associated with the Andean Patagonian forests and usually belong to National Parks or protected areas. They are accompanied by a large number of small and shallow oligotrophic lakes, comprising an important lacustrine area (Quirós and Drago 1999). The underwater light climate of several North Patagonian lakes has been previously studied (Pérez et al. 2002; Pérez 2006). These investigations revealed that some shallow lakes belong to the *G* (*gilvin*) type, according to the classification proposed by Kirk (2011), due to the dominance of CDOM as the principal light absorbing component. In particular, the shallow neighboring Lake Escondido and Lake Morenito, with 0.08 and 0.38 km^2 surface area, respectively, have roughly similar nutrient concentration but different dissolved organic carbon (DOC) concentrations (Morris et al. 1995; Bastidas Navarro et al. 2009). The lakes also registered different light attenuation coefficients of blue and green light during a summer survey with Lake Morenito being more transparent for both wavelengths (Pérez et al. 2002; Pérez 2006). Moreover, Bastidas Navarro et al. (2009) found that the ratio between the abundances of PE-rich in relation to the PC-rich picocyanobacteria (PE:PC) was higher in the more transparent Lake Morenito compared to Lake Escondido. These authors suggested that this result could be related to differences in the spectral composition of underwater light shaped by different DOM concentrations.

In this context, these two lakes offer an excellent natural scenario to assess the temporal dynamic of CDOM in relation to precipitation patterns and its effects on phytoplankton community structure due to differences in underwater light climate. Thus, we performed a synchronized sampling of these two shallow neighbor lakes during an annual cycle in order to evaluate (1) how CDOM affected the underwater light climate of both lakes in relation to the precipitation regime, and (2) the influence of the underwater light climate (light intensity and spectral composition) on nano- and microphytoplankton community structure.

Materials and methods

Study site

Escondido and Morenito are two shallow, oligotrophic lakes located in the Nahuel Huapi National Park, Patagonia, Argentina. Lake Escondido is located 3.7 km east from Lake Morenito and is smaller and slightly shallower compared to Lake Morenito (Online Resource 1, 2). Both lakes have glacial origin and are surrounded by mixed forests of *Nothofagus dombeyi* and *Austrocedrus chilensis*.

Both lakes are continuously cold polymictic, and occasionally freeze (Balseiro and Modenutti 1990; Queimaliños 2002). The chlorophyll *a* (Chl*a*) concentration ranges between 0.5 and 2.8 μg L^{-1} in Lake Escondido (Diaz and Pedrozo 1993; Bastidas Navarro et al. 2009; Pérez et al. 2010), while in Lake Morenito the concentrations range between 1.0 and 3.6 μg L^{-1} (Modenutti et al. 2000; Bastidas Navarro et al. 2009). The DOC concentration varies between 2.7 and 5.4 mg L^{-1} in Lake Escondido (Morris et al. 1995; Bastidas Navarro et al. 2009; Pérez et al. 2010) and between 1.8 and 3.3 mg L^{-1} in Morenito (Alonso et al. 2004; Bastidas Navarro et al. 2009). Lake Escondido is the only water body in a closed small subbasin (seepage). In contrast, Lake Morenito is situated in an open basin, and is connected upstream with Ezquerra pond and downstream with Lake Moreno West (Online Resource 2). In this context, both lakes lack inlet streams. The climate of this region is cold temperate with a mean annual precipitation around 1,800 mm (Rapacioli 2011), with the rainy period (73 % of the annual precipitation) in austral fall and winter seasons (April–September), and a dry spring–summer season (October–March) (Jobbágy et al. 1995; Paruelo et al. 1998).

Sample collection

The study period spanned 13 months from January 2010 to January 2011. Samples were obtained every month, except in March, August and December, resulting in a sampling schedule of ten different dates. Both lakes were sampled the same day consecutively. Water samples were taken using a 12-L Schindler–Patalas trap, at a sampling point located over the deepest part of each lake. Four depths were sampled: 0, 3 and 6 m for both lakes, and the fourth depth was 7 m for Lake Escondido and 8 m for Lake Morenito. Samples were transferred to 5-L polypropylene containers, which were acid-washed and pre-rinsed before sampling. Samples were carried in darkness to the laboratory within 2 h of collection. Temperature, pH and dissolved oxygen concentration were measured in situ with a Hanna HI98150 and Hanna HI9142 portable meter (Hanna Instruments, Woonsocket, RI, USA). Conductivity was measured in situ with an Orion (Model 115) portable meter.

Laboratory analyses

Optically active substances [i.e., total suspended solids (TSS), CDOM and Chl*a*] were determined in the laboratory. Particles were collected onto pre-combusted and preweighed GF/F filters used to measure the TSS dry weight (APHA 2005). Absorption by CDOM was characterized by UV–visible spectrophotometric scans performed on filtered lake water (through pre-combusted GF/F filters), therefore CDOM absorption values correspond to the dissolved organic fraction smaller than ~0.2 μm. The nominal pore size of GF/F filters decreases with the pre-combustion process reducing the particle cutoff size (Nayar and Chou 2003; Asmala et al. 2012). It is worthy to mention that in two sampling dates samples were filtered using both GF/F pre-combusted filters and membrane 0.2 μm filters, and the results were similar (difference <5 %).

We focused on two optical parameters: (1) the CDOM spectral absorption coefficient [$a_{CDOM}(\lambda)$] and (2) the spectral slope between 275 and 295 nm ($S_{275–295}$) as a proxy of the CDOM molecular size (Helms et al. 2008). Absorbance was determined in filtered natural water with a Hewlett Packard 8453 diode array spectrophotometer, using a 10 cm quartz cuvette and recording absorbance between 200 and 800 nm at 1 nm intervals against a blank of ultrapure water. The average absorbance from 700 to 800 nm was subtracted from each spectrum to correct for offsets due to several instrument baseline effects like residual scattering, temperature differences and instrument drift (Green and Blough 1994; Helms et al. 2008). Absorbance units were converted to absorption coefficients as follows (Kirk 2011):

$$a_{CDOM}(\lambda) = 2.303 \frac{A(\lambda)}{l} \quad (1)$$

where $a_{CDOM}(\lambda)$ is the Napierian absorption coefficient, A the absorbance, and l is the path length (m). The spectral slopes $S_{275–295}$ were calculated by fitting a linear regression (LR) to the log-transformed spectra, and reported as a positive number. Chl*a* concentrations were determined spectrophotometrically by extraction with 90 % ethanol following Nusch (1980). The $a_{CDOM}(440)$:Chl*a* ratio was used as an allochthonous CDOM indicator following Webster et al. (2008) and Queimaliños et al. (2012). This ratio is an index of terrigenous organic carbon relative to endogenous producer biomass, which increase when terrestrial CDOM enters to the lake.

Nutrient concentrations were determined on the soluble fraction by passing water through precombusted GF/F filters. The dissolved fractions included total dissolved

phosphorus (TDP), soluble reactive phosphorus (SRP) and total dissolved nitrogen (TDN). Nutrient fractions that included particulate matter were determined by analyzing unfiltered samples. This included total phosphorus (TP) as well as total nitrogen (TN). TP and TDP were determined by digesting samples with potassium persulfate at 125 °C and 1.5 atm for 1 h. The concentrations were determined through the ascorbate-reduced molybdenum method followed by spectrophotometric reading (APHA 2005). In the case of SRP the concentration was obtained through the same method but without persulfate digestion (APHA 2005). For determination of TN and TDN, the samples were digested with potassium persulfate in sodium hydroxide at 125 °C and 1.5 atm for 1 h. The concentrations were obtained through the acidification of the sample with concentrated sulfuric acid before the spectrophotometric reading (Bachmann and Canfield 1996).

Optical model and light attenuation

Due to the fact that during several sampling dates wind action and scattering or varying cloudiness led to significant noise to in situ light versus depth measurements, determination of spectral light attenuation was not always precise. Unfortunately, a reference sensor held above water was not available during sampling. Therefore, in order to have a comprehensive temporal characterization of underwater light climate we followed two different approaches. On the one hand, considering that in oligotrophic lakes underwater light transmission is frequently primarily controlled by CDOM concentration, water transparency was inferred from CDOM absorption coefficients for the reference wavelength 440 [$a_{CDOM}(440)$]. On the other hand, we modeled the diffuse attenuation coefficient using Kirk's optical model (Kirk 1981, 1984, 1994) (see Eq. 2). The model relates the average value of the vertical attenuation coefficient for downward irradiance in the euphotic zone as an explicit function of a, b, and μ_0 as follows:

$$\mathrm{Kd}(\lambda) = \frac{1}{\mu_0}\left[(a_t)^2 + G(\mu_0)a_t(\lambda)b(\lambda)\right]^{0.5} \quad (2)$$

where μ_0 is the average cosine of the angle of the stream of photons just under the surface (calculated from the incident zenith angle using Snell's law), $G(\mu_0)$ is a coefficient that indicates the relative contribution of scattering to vertical attenuation of irradiance and it is determined by the shape of the volume scattering function [$\beta(\theta)$] and by μ_0. $G(\mu_0)$ is a linear function of μ_0 in accordance of: $G(\mu_0) = g_1 \cdot \mu_0 - g_2$. The constants g_1 and g_2 are values that vary with the shape of volume scattering function used by in the calculations (Kirk 1991). We used the coefficients $g_1 = 0.425$ and $g_2 = 0.19$, estimated from San Diego Harbor scattering phase function (Kirk 2011), which are adequate for current purposes because it is not very sensitive to the scattering phase function in waters with a relatively high absorption to scattering ratio. Total spectral absorption coefficient [$a_t(\lambda)$] is the sum of CDOM absorption [$a_{CDOM}(\lambda)$], phytoplankton absorption [$a_{ph}(\lambda)$], unpigmented particulate absorption [$a_d(\lambda)$], and pure water absorption coefficient [$a_w(\lambda)$]. Finally, $b(\lambda)$ is the total scattering coefficient (i.e., particle scattering coefficient + water scattering coefficient).

To apply Kirk's optical model, phytoplankton spectral absorption was estimated as the product of specific phytoplankton absorption coefficient [$a_{ph}^*(\lambda)$] and measured Chl*a* concentration. Previously reported values of $a_{ph}^*(\lambda)$ by Pérez et al. (2002) and Pérez (2006), for each lake, were used. Similarly, unpigmented particulate spectral absorption was estimated as the product of specific unpigmented absorption coefficient [$a_d^*(\lambda)$] and TSS concentration. Values of $a_d^*(\lambda)$ for each lake were obtained from Pérez (2006). The absorption coefficient for pure water was taken from Pope and Fry (1997). In addition, spectral scattering coefficient of particles [$b_p(\lambda)$], was calculated from TSS values following Gallegos (2001):

$$b_p(\lambda) = d \cdot \mathrm{TSS}\left(\frac{550}{\lambda}\right) \quad (3)$$

where the coefficient d was obtained from the regression analysis of turbidity against TSS for both lakes ($b = 0.30$ and $b = 0.34$ for Lake Escondido and Morenito, respectively) (G.L. Pérez, unpublished data), the $550/\lambda$ term introduces the inverse wavelength dependence of scattering coefficient suggested by Morel and Gentili (1991). Spectral scattering coefficient of pure water [$b_w(\lambda)$] was taken from Smith and Baker (1981). We also made the calculations restricted to the abiotic component of light attenuation (i.e., CDOM absorption, pure water and the average cosine of downwelling irradiance), obtaining an "abiotic" Kd(λ) (KdAbio), in order to evaluate the importance of the biotic and abiotic component in the attenuation of light.

Subsequently, Kirk's model was used to partition light attenuation coefficient and to determine the relative contribution of absorption and scattering of different components to light attenuation. Following procedures set forth by Belzile et al. (2002), the relative contribution of inherent optical properties to Kd were examined by calculating different optical scenarios representing fractionated contributions of absorption and scattering by particles, or by CDOM and pure water, to total Kd(λ) (see optical conditions of different models applied by Belzile et al. 2002).

Additionally, absorption budget was directly estimated from mean spectral absorption of different components (i.e., CDOM, phytoplankton, unpigmented particles and

pure water) in the water column. Absorption budget was calculated as the contribution (in percentage) of each component to total spectral absorption. To estimate PAR, spectra were integrated between 400 and 700 nm.

After modeling the spectral dependence of the attenuation coefficient, the downwelling component of the light field at a given depth can be estimated from the value of irradiance immediately below the surface of the water column as follows:

$$\mathrm{Ed}(Z,\lambda) = \mathrm{Ed}(0-,\lambda)\cdot\exp[-\mathrm{Kd}(\lambda)\cdot Z] \quad (4)$$

where Ed(Z, λ) is the downwelling irradiance at depth Z and wavelength λ, Ed(0−, λ) the measured subsurface irradiance at wavelength λ converted from energy units (W m^{-2} nm^{-1}) to quantum units (μmol photons m^{-2} s^{-1} nm^{-1}) (see validation of Kirk's Model), Kd(λ) the modeled attenuation coefficient for downwelling irradiance at wavelength λ, and Z is the depth. Then the broadband modeled Kd(PAR) was calculated by propagating the numerically integrated solar spectrum just below the surface, Ed(0−, λ) in quantum units, to a reference depth following a general procedure (i.e., Gallegos 1994; Belzile et al. 2002):

$$\mathrm{Kd(PAR)} = -\frac{1}{Z}\cdot\mathrm{Ln}\left(\frac{\int_{400}^{700}\mathrm{Ed}(\lambda,0-)\exp[-\mathrm{Kd}(\lambda)\cdot Z]\mathrm{d}\lambda}{\int_{400}^{700}\mathrm{Ed}(\lambda,0-)\mathrm{d}}\right) \quad (5)$$

Validation of Kirk's model

Comparisons of measured (obtained without significant cloud cover) and modeled spectral light attenuation in both lakes were carried out in a set of eight spectra. Underwater vertical profiles of spectral (380–750 nm) downward irradiance [Ed(λ, Z)] were performed around noon (±1.5 h) on each sampling occasions, using a calibrated USB2000 (Ocean Optics) spectroradiometer (1.5 nm bandwidth FWHM) attached to a fiber optic probe with a CC-3-UV-T cosine corrected diffuser yielding 180° field of view. The spectral vertical diffuse attenuation coefficient [Kd(λ)] was determined from the slope of the LR of the natural logarithm of Ed(λ) versus depth. Values of Ed(λ, Z) were converted from energy units (W m^{-2} nm^{-1}) to quantum units (μmol photons m^{-2} s^{-1} nm^{-1}) and the broadband attenuation coefficient for PAR band [Kd(PAR)] was calculated applying Eq. 5.

We found a good agreement between measured and modeled spectral light attenuation coefficient between 400 and 700 nm (see Online Resource 3). Results showed low mean values (<20 %) of relative root mean square error (RRSME) and high mean values (>0.85) of similarity coefficient (SC) (see Online Resource 4 for further explanation of errors calculations and statistics). For PAR band and reference wavelengths 440, 550 and 675 nm we found a significant linear relationship between modeled and measured Kd values, with $R^2 > 0.91$ and near 1:1 relationships (mean regression slope varying between 0.9 and 1.07).

Characterization of underwater light climate

We used modeled spectral attenuation coefficients to describe light attenuation and spectral distribution of downward irradiance throughout the water column of Lakes Escondido and Morenito during the study period. The corresponding Kd for different colors: blue [Kd(BLUE)], green [Kd(GREEN)] and red [Kd(RED)], were calculated at 440, 550 and 675 nm, respectively. Differences in spectral composition of underwater light climate were estimated by the relative changes of attenuation coefficients at reference wavelengths [i.e., the ratio between Kd(RED) and Kd(GREEN)] (Vörös et al. 1998), this metric being indicative of the spectral dominance of the underwater light climate, hereafter Kd(R)/Kd(G) ratio.

Light availability in the pelagic zone was calculated as the mean daily irradiance of the water column for the PAR band [Ed(Z_{mean}, PAR)], representing the average exposing intensity for algae in complete mixing, following (Ferrero et al. 2006):

$$\mathrm{Ed}(Z_{\mathrm{mean}},\mathrm{PAR}) = \mathrm{Ed}(0-,\mathrm{PAR})\frac{1-\exp[-\mathrm{Kd(PAR)}Z]}{[\mathrm{Kd(PAR)}Z]} \quad (6)$$

where Ed(0−, PAR) is the mean daily incident irradiance for PAR band calculated from solar radiation recorded with a GUV 511 radiometer (Biospherical Instruments, Inc.) located at the laboratory (~17 km from sampling sites) after correction for the transmission through the air–water interface (transmission factor 0.97), Kd(PAR) is the modeled vertical diffuse attenuation coefficient for PAR band and Z is water column depth in the sample site. Additionally, spectral mean irradiance of the water column [Ed(Z_{mean}, λ)] was calculated around noon with the same equation described above using the subsurface spectral irradiance [Ed(0−, λ)] recorded with USB2000 (Ocean Optics) spectroradiometer and the modeled spectral attenuation coefficient Kd(λ). The euphotic depth (Z_{euph}), the depth at which PAR falls to 1 % of its value just under the surface, was calculated as: $Z_{euph} = 4.605/\mathrm{Kd(PAR)}$.

Precipitation data

The temporal variation in precipitation was obtained from hydrometeorological reports published by the AIC

(Autoridad Interjurisdiccional de Cuencas, Río Negro, Argentina) (AIC 2011), with data collected at a meteorological station located approximately 1.1 km to the South of Lake Escondido and 3.8 km to the South West of Lake Morenito. To explore the influence of precipitation on $a_{CDOM}(440)$ in the lakes, we calculated the cumulative precipitation at different time periods. For this, we followed a simple approach: for each sampling date we calculated the cumulative precipitation as the sum of the daily rainfall (mm) data, from 30 to 360 days before sampling date (using intervals of 30 days).

Nano- and micro-phytoplankton composition, abundance and biomass

Phytoplanktonic taxa were identified following previous studies performed in these same lakes (Diaz and Pedrozo 1993; Queimaliños 1993, 2002). We classified the phytoplankton taxa either as autotrophic or mixotrophic depending on their phagotrophic capability, according to previous grazing experiments (Sanders and Porter 1988; Tranvik et al. 1989; Jones 1994; Queimaliños 2002).

Samples for photosynthetic nanoplankton (2–20 μm) quantification were fixed with ice-cold filtered glutaraldehyde 10 % (final concentration 1 %). A volume between 10 and 25 mL of each fixed sample was stained with 10 μg mL^{-1} (final concentration) of 4′,6-diamidino-2-phenylindole (DAPI) according to Porter and Feig (1980), and then filtered through a 0.8 μm black polycarbonate membrane filter (Millipore). Filters were mounted on a microscope slide with a drop of immersion oil for fluorescence microscopy (Immersol 518 F) and stored at −20 °C. For cell quantification, samples were inspected at 1,000× magnification using an epifluorescence microscope (Olympus BX50, Japan) using an HBO 50W lamp and a filter set for blue light excitation (BP 420–480 nm, BA 515 nm), green light excitation (BP 480–550 nm, BA 590 nm) and UV excitation (BP 330–385 nm, BA 420 nm). Flagellates smaller than 20 μm were inspected under blue light excitation in order to identify the presence of chlorophyll autofluorescence, thus, preventing confusion with heterotrophic nanoflagellates.

The microphytoplankton (>20 μm) were counted following the Utermöhl technique, for which additional water samples were fixed with acid Lugol's solution and counted under an inverted microscope (Olympus CKX41, Japan) using 50 mL Utermöhl chambers. Microphytoplankton were quantified by scanning the entire chamber surface at 400× magnification. Cell abundance of both size fractions was determined for each sample. For simplicity nano- and microphytoplankton will be referred to as phytoplankton.

The size of at least 30 cells of each phytoplankton taxon was measured under the microscope using an ocular micrometer. The biovolume (μm^3) of each taxon was estimated by applying the geometric models proposed by Sun and Liu (2003). To convert the phytoplankton biovolume into carbon biomass, we employed the conversion factor proposed by Menden-Deuer and Lessard (2000), as follows: Dinoflagellates: pg C $cell^{-1} = 0.760$ pg $(\mu m^3\ cell^{-1})^{0.819}$; Diatoms: pg C $cell^{-1} = 0.288$ pg $(\mu m^3\ cell^{-1})^{0.811}$; other algae: pg C $cell^{-1} = 0.216$ pg $(\mu m^3\ cell^{-1})^{0.939}$. The total carbon biomass was calculated for each taxon by multiplying the taxon biomass by their abundance. For the analysis, we considered the phytoplankton taxa which contributed more than 5 % of the total phytoplankton biomass.

Statistical analyses

Considering that both lakes are polymictic and the assessed variables showed low variability along the water column, we focused on the analysis of the differences between lakes comparing the mean values of physicochemical, biological and optical properties of the water column throughout the study period. We performed two-way RM ANOVA tests (using the Holm–Sidak method for multiple comparisons) with Lake and sampling time as main factors. When differences between lakes in both Kd(PAR) and Kd(R)/Kd(G) ratio were analyzed, two-way ANOVA tests (using the Holm–Sidak method for multiple comparisons) were utilized.

To analyze the effect of cumulative precipitation on $a_{CDOM}(440)$ dynamics in each studied lake, we performed a stepwise, forward multiple linear regression (MLR) analysis. The MLR were performed with $a_{CDOM}(440)$ as dependent variable and the different intervals (of 30 days) for the cumulative precipitation from 30 to 360 days before sampling (e.g., 30, 60, 90,…360 days) as independent variables. With this procedure we searched for the cumulative precipitation interval with the best fit.

Pearson correlation (CA) or simple LRs analyses were performed to analyze the relationships among the studied variables (optical, biological and physicochemical) as well as the temporal synchrony between lakes for a given variable. The effect of variables as potential drivers explaining differences in phytoplankton community structure was assessed by both LR and MLR analyses. The MLR were performed with Cryptophyceae and Chrysophyceae biomass as dependent variables and the physicochemical (temperature, conductivity, DO, TSS, TDN, TN, TDP, TP, SRP) and optical variables [$a_{CDOM}(440)$, Ed(Z_{mean}, PAR), Kd(PAR), Kd(R)/Kd(G) ratio] as independent variables. We also made the analysis with KdAbio(PAR) and KdAbio(R)/KdAbio(G) ratio, which were estimated applying Eq. 2 and were used as independent variables. In all MLR analyses, the multicollinearity was

assessed by computing the variance inflation factors (VIFs).

The sample sizes varied according to the analysis performed. For the evaluation of synchrony between lakes of the $a_{CDOM}(440)$ and $S_{275–295}$ the sample size was $n = 40$. When the CA, LR and MLR analyses involved either optical variables [Ed(Z_{mean}, PAR), Kd(PAR), Kd(R)/Kd(G) ratio] or cumulative precipitation periods that presented a unique value for each sampling date, the sample size was $n = 10$ (when one lake was considered) and $n = 20$ (when both lakes were analyzed together). When LR analyses involved relationships between modeled light attenuation and CDOM absorption coefficients, the sample size was $n = 8$ in order to avoid circularity in the analysis. The sample size corresponds to the 8 low-noise measurements of Kd(λ).

Prior to each analysis, the Kolmogorov–Smirnov test and Spearman rank correlation were run in order to test the data for normality and homoscedasticity, respectively. Whenever the data did not conform, the values were log transformed.

Results

Environmental characterization

The physicochemical variables measured in both lakes are summarized in Table 1. Both lakes showed similar dynamics in water temperature and nutrient concentrations throughout the year. The water column was completely mixed during most of the year, with a mild stratification at late October and November in Lake Morenito and at February in Lake Escondido. The minimum winter temperature was 5 °C and the summer maximum was about 20 °C in both lakes (Table 1). Nutrient concentrations were very low in both lakes, confirming their oligotrophic status. Both lakes showed mean TN concentrations around 400 μg L^{-1} and mean TP concentrations around 10 μg L^{-1}. The concentration of different fractions of phosphorus and nitrogen were similar in both lakes (Table 1).

Conductivity was significantly different between lakes (Table 1). In contrast, no differences were found in dissolved oxygen, pH, and TSS (Table 1). Both environments were well oxygenated and the pH remained near neutrality throughout the water column. Mean Chl*a* concentration was similar in both lakes, with values of 1.13 ± 0.5 and 1.24 ± 0.4 μg L^{-1} for Lake Escondido and Morenito, respectively (Table 1). Maximum values of mean Chl*a* were observed during May for Lake Escondido and during September for Lake Morenito. The temporal variation of Chl*a* did not fluctuate synchronously among the lakes throughout the year.

CDOM characterization and allochthonous indicators

Values of $a_{CDOM}(440)$ were always almost threefold greater in Lake Escondido than in Lake Morenito (Table 1; Fig. 1a), with significant differences between lakes depending on sampling time (interaction was significant) (two-way RM ANOVA: Lake, $F = 10.20$, $p < 0.001$). Differences in $a_{CDOM}(440)$ between lakes were significant in January–February and July–November. Maximum values of $a_{CDOM}(440)$ were observed in September and October for Lake Escondido and Lake Morenito, respectively (Fig. 1a). A synchronous variation of the $a_{CDOM}(440)$ between lakes was observed throughout the studied period (CA: $R = 0.520$, $p < 0.001$, $n = 40$). For both lakes, variation of $a_{CDOM}(440)$ was significantly explained by the cumulative precipitation of 150 days before sampling, according to the stepwise forward model regression applied. In the case of Lake Escondido the model yielded: $a_{CDOM}(440) = 0.000839 \times 150$ days $+ 0.875$ (MLR: $R^2 = 0.801$, $p < 0.001$, $n = 10$). For Lake Morenito the model yielded: $a_{CDOM}(440) = 0.000294 \times 150$ days $+ 0.343$ (MLR: $R^2 = 0.446$, $p = 0.035$, $n = 10$) (Fig. 1a).

The $S_{275–295}$ values were always significantly lower in Lake Escondido than in Lake Morenito (two-way RM ANOVA: Lake, $F = 508.5$, $p < 0.001$) (Table 1). Differences between lakes did not depend on sampling time. Synchronous fluctuation in $S_{275–295}$ was observed between lakes (CA: $R = 0.899$, $p < 0.001$, $n = 40$). In contrast to $a_{CDOM}(440)$, temporal variation in $S_{275–295}$ exhibited minimum values during September. The $a_{CDOM}(440)$:Chl*a* ratio was significantly different between lakes (two-way RM ANOVA: Lake, $F = 1{,}126.8$, $p < 0.001$). Lake Escondido showed higher $a_{CDOM}(440)$:Chl*a* ratios than Morenito throughout the studied period (Table 1).

Light attenuation dynamics

Assessing the underwater light climate with Kirk's optical model (Eq. 2), we always observed higher modeled Kd(PAR) values in Lake Escondido than in Lake Morenito (Table 1; Fig. 1b). Differences between lakes were significant (two-way ANOVA: $F = 54.5$, $p < 0.001$) and did not depend on sampling time. In both lakes the euphotic zone was near or in excess of water column depth (Table 1). Regarding seasonal variation, maximum values of Kd(PAR) were observed during September in Lake Escondido [Kd(PAR) = 0.671 m^{-1}] and during June in Lake Morenito [Kd(PAR) = 0.478 m^{-1}] (Fig. 1b). Non-significant relationship was observed for Kd(PAR) values between lakes, showing no synchronous variation. In Lake Escondido temporal variation of Kd(PAR) strongly

Table 1 Physicochemical, biological and optical characterization of the studied lakes

	Lake Escondido		Lake Morenito	
	Mean ± SD	Range	Mean ± SD	Range
Physicochemical and biological properties				
Temperature (°C)	12.21 ± 5.58	5.0–21.4	12.48 ± 4.97	5.0–19.9
TSS (mg L^{-1})	0.42 ± 0.36	0.10–1.57	0.50 ± 0.43	0.10–1.38
TP (μg L^{-1})	7.62 ± 2.43	3.48–13.23	8.80 ± 2.61	4.28–17.06
TDP (μg L^{-1})	4.95 ± 1.19	2.65–7.36	4.82 ± 1.34	2.44–8.05
SRP (μg L^{-1})	3.21 ± 1.30	1.07–5.00	2.34 ± 0.91	0.13–5.06
TN (μg L^{-1})	383.95 ± 91.15	270.09–623.9	450.0 ± 121.9	246.5–765.3
TDN (μg L^{-1})	347.61 ± 82.45	246.0–578.0	333.2 ± 88.5	207.2–564.3
Conductivity (μS cm^{-1})*	63 ± 3	57–70	70 ± 3	59–75
pH	7.3 ± 0.4	6.3–7.8	7.3 ± 0.5	6.5–8.0
Dissolved oxygen (mg L^{-1})	11.12 ± 1.26	8.90–12.50	11.09 ± 1.46	9.0–13.0
Chl*a* (μg L^{-1})	1.13 ± 0.5	0.4–2.7	1.24 ± 0.4	0.6–2.4
$a_{CDOM}(440)$:Chl*a* [m^{-1} (μg $L^{-1})^{-1}$]*	1.367 ± 0.707	0.684–2.843	0.398 ± 0.116	0.260–0.588
Optical properties				
$a_{CDOM}(320)$ (m^{-1})*	9.631 ± 1.376	7.637–11.518	3.879 ± 0.403	3.338–4.245
$a_{CDOM}(340)$ (m^{-1})*	7.096 ± 1.030	5.623–8.478	2.740 ± 0.310	2.273–3.028
$a_{CDOM}(440)$ (m^{-1})*	1.260 ± 0.195	0.979–1.562	0.481 ± 0.080	0.330–0.581
$S_{275–295}$ (10^{-3} nm^{-1})*	17.13 ± 1.02	15.50–19.20	20.69 ± 1.29	17.90–23.00
Kd(PAR) (m^{-1})*	0.550 ± 0.060	0.441–0.652	0.346 ± 0.058	0.288–0.445
Kd(BLUE) (m^{-1})*	3.027 ± 1.083	1.368–4.459	1.273 ± 0.512	0.596–2.077
Kd(GREEN) (m^{-1})*	0.844 ± 0.340	0.354–1.348	0.443 ± 0.223	0.206–0.809
Kd(RED) (m^{-1})	1.236 ± 0.473	0.655–1.919	1.180 ± 0.499	0.626–2.026
Kd(R)/Kd(G) ratio*	1.498 ± 0.231	1.129–1.849	2.706 ± 0.365	2.247–3.241
Ed(Z_{mean}, PAR) (μmol photons m^{-2} s^{-1})	222.75 ± 110.9	77.36–378.3	288.4 ± 140.1	100.8–474.8
Z_{euph} (m)	8.34 ± 1.10	6.86–10.54	13.18 ± 2.06	9.63–15.77

SD standard deviation

* Significant differences between lakes were analyzed for each variable through two-way ANOVA; $p < 0.05$

followed $a_{CDOM}(440)$ variation. However, in Lake Morenito the highest Kd(PAR) was not coincident with the maximum $a_{CDOM}(440)$ value (Fig. 1a, b). During October, higher solar altitude ($\mu_0 = 0.897$) relative to June ($\mu_0 = 0.741$) decreased light attenuation by about 15 % in Lake Morenito. On the other hand, considering measured values of Kd(PAR) and both lakes together, variation in light attenuation was significantly explained by differences in $a_{CDOM}(440)$ (LR: $R^2 = 0.84$, $p < 0.001$, $n = 8$).

Regarding light availability in the water column, mean daily irradiance for PAR was similar between lakes (Fig. 1c; Table 1), showing lower difference than observed for Kd(PAR). During the study period, mean value of Ed(Z_{mean}, PAR) was 1.29-fold higher in Lake Morenito compared to Lake Escondido. Temporal dynamics of Ed(Z_{mean}, PAR) showed minimum values from June to September and the maximum from November to February (Fig. 1c), varying synchronously between lakes (CA: $R = 0.93$, $p < 0.001$, $n = 10$).

Spectral composition of underwater light

Clear differences in modeled light attenuation at reference wavelengths were observed between lakes (Fig. 1d). Lake Morenito always showed higher Kd(R)/Kd(G) ratio than Lake Escondido (two-way ANOVA: $F = 164.7$, $p < 0.001$). Differences between lakes did not depend on sampling time. Mean value of Kd(R)/Kd(G) ratio was 2.7 for Lake Morenito and 1.5 for Lake Escondido (Table 1; Fig. 1d). Minimum values of Kd(R)/Kd(G) ratio were registered from July to November for Lake Escondido and from June to November for Lake Morenito. Maximum values were observed either from May to June of 2010 or from January to February of 2011 for Lake Escondido. For Lake Morenito, maximum values were observed either from January to April of 2010 or from January to February of 2011 (Fig. 1d). No significant synchronous variation throughout the studied period was observed for Kd(R)/Kd(G) ratio between lakes. In Lake Escondido temporal variation in

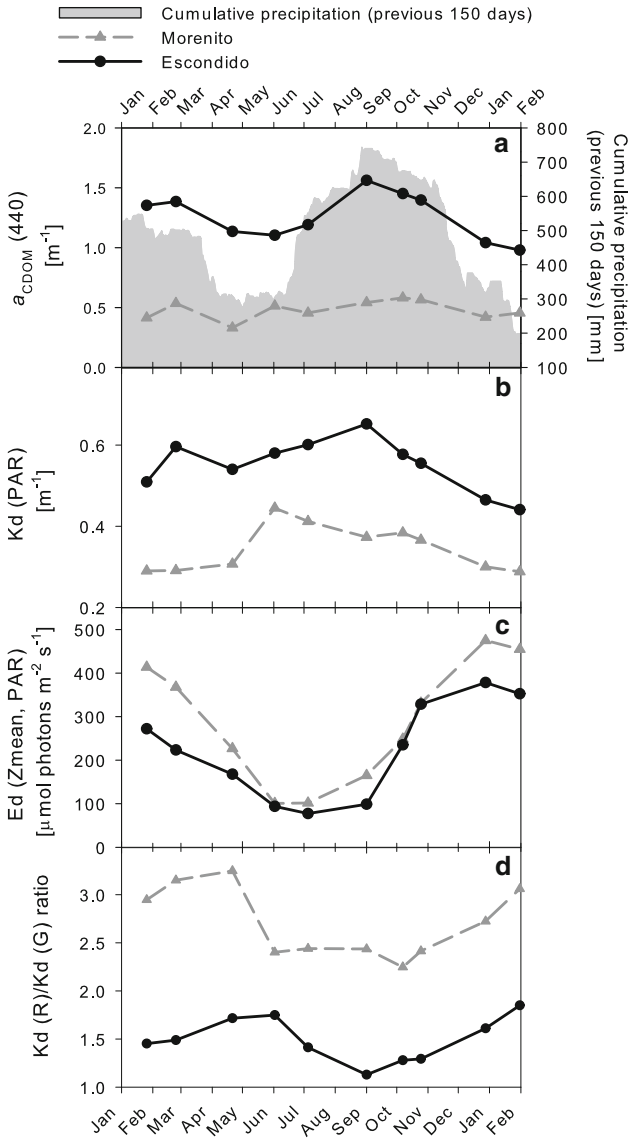

Fig. 1 Seasonal variation of optical variables and precipitation in the studied lakes. **a** 150 days of cumulative precipitation (mm) before sampling date (*grey area*) and the mean water column absorption coefficient of colored dissolved organic matter at 440 nm [$a_{CDOM}(440)$]; **b** the attenuation coefficient for PAR [Kd(PAR)]; **c** mean daily irradiance [Ed(Z_{mean}, PAR)]; and **d** the ratio of red to green light [Kd(R)/Kd(G) ratio]

Kd(R)/Kd(G) ratio strongly followed, in an opposite trend, differences in $a_{CDOM}(440)$. Meanwhile, in Lake Morenito this pattern was less evident, although minimum values of Kd(R)/Kd(G) ratio were coincident with $a_{CDOM}(440)$ maximum and highest Kd(R)/Kd(G) ratios occurred generally at low $a_{CDOM}(440)$ values (Fig. 1a, d). Regarding spectral attenuation signature between 400 and 700 nm, Kd(λ) always showed higher values at blue and red ends of the spectra. Both lakes presented minimum values of Kd(λ) in the 550–580 nm spectral region (Fig. 2a, d). On the other hand, considering measured values of Kd(λ) and both lakes together, variation in Kd(R)/Kd(G) ratio was significantly explained by differences in $a_{CDOM}(440)$ (LR: $R^2 = 0.80$, $p < 0.001$, $n = 8$).

Regarding absorption budget, both lakes showed a major contribution to total light absorption by CDOM (mainly in the blue spectral region) and by water itself (mainly in the red spectral region), since the contribution of particulate absorption were comparatively less important (Fig. 2b, e). Contribution of CDOM to total absorption in the broad-band PAR was higher in Lake Escondido than Lake Morenito, with a mean value of 75.8 %. Instead, Lake Morenito showed a mean contribution of CDOM to total light absorption of 54.4 %.

Partitioning Kd(PAR) applying Eq. 2 was used to calculate the relative contribution of scattering and absorption in the attenuation mechanism for PAR (see "Optical model and light attenuation"). Results showed that absorption by CDOM and water itself contributed to Kd(PAR) on average 52.2 and 37.2 %, respectively, in Lake Morenito, and 74.1 and 20.4 %, respectively, in Lake Escondido. Regarding particles, absorption and scattering of this fraction only contributed with 7.3 and 3.3 % of Kd(PAR), respectively, in Lake Morenito, and 3.8 and 1.7 %, respectively, in Lake Escondido. Differences in the relative contribution of CDOM absorption to light attenuation resulted in dissimilar spectral composition of Ed(λ, Z) between lakes. In Lake Escondido, downward irradiance around 550 nm typically showed a strong decrease and the spectral composition shifted towards green–yellow light (570–585 nm) [i.e., lower values of Kd(R)/Kd(G) ratio] (Fig. 2c). In Lake Morenito, downward irradiance between 550 and 570 nm penetrated deepest and the spectral composition of the downwelling flux changed progressively with increasing depth resulting in an underwater light field dominated by green light [i.e., higher values of Kd(R)/Kd(G) ratio] (Fig. 2f).

Concerning spectral composition of mean Ed(Z_{mean}, λ), differences between lakes were evident if dates of lowest Kd(R)/Kd(G) ratio for Lake Escondido and highest Kd(R)/Kd(G) ratio for Lake Morenito were compared (Fig. 3). Lake Morenito presented an average underwater light field largely dominated by green light with a maximum value around 565 nm ($\sim$3 µmol photons m^{-2} s^{-1}). In contrast, Lake Escondido had an underwater light field dominated by green–yellow light with a maximum value around 585 nm ($\sim$1.5 µmol photons m^{-2} s^{-1}) (Fig. 3a). The maximum difference of Ed(Z_{mean}, λ) between lakes was observed in the 550–580 nm band, because this spectral region was strongly attenuated in Lake Escondido (Fig. 3).

Phytoplankton community composition, abundance and biomass

The phytoplankton community of both lakes was composed of mixotrophic and autotrophic taxa (Table 2). Total

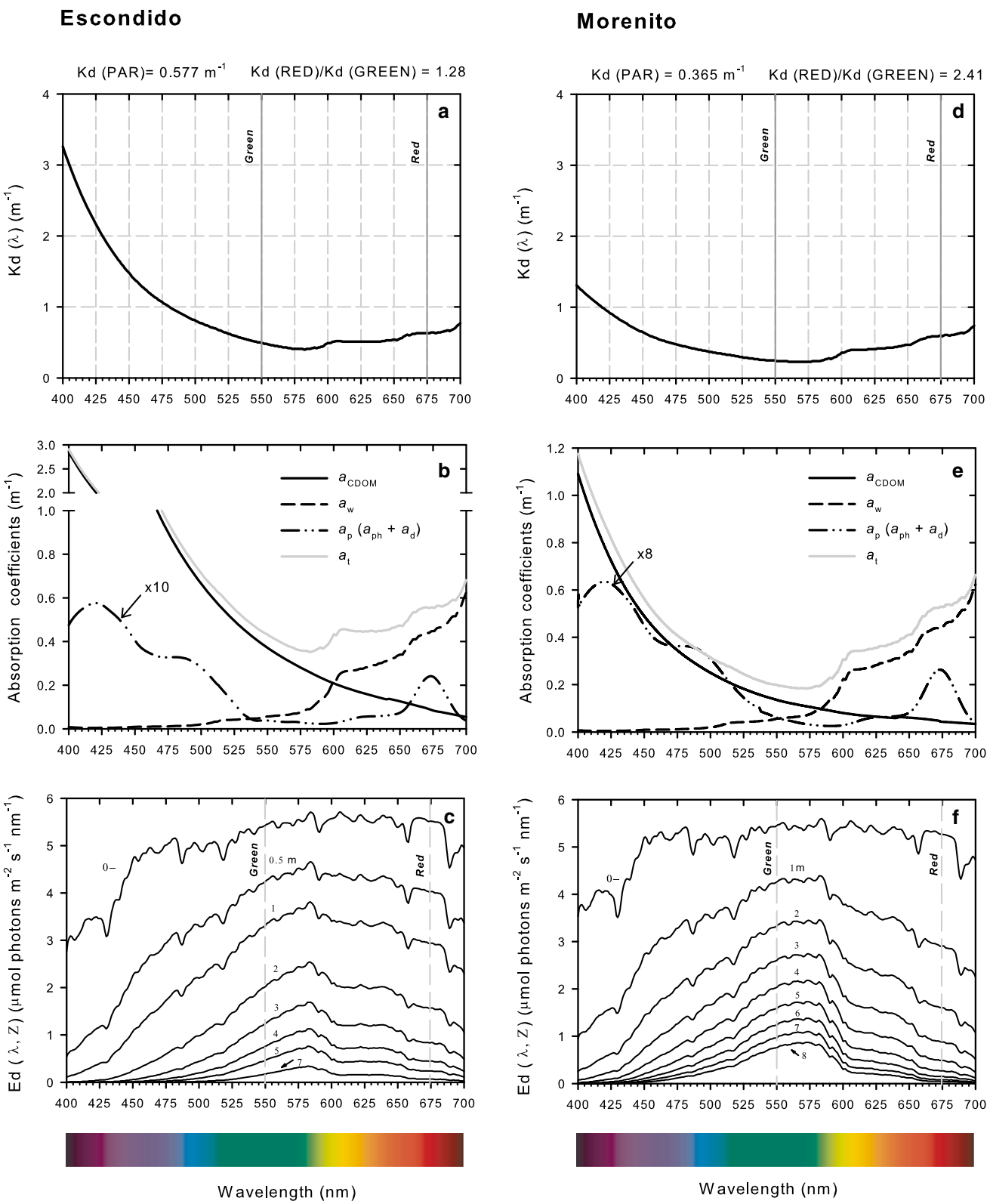

Fig. 2 Optical properties and underwater light climate of sampling dates showing the most representative optical situations observed during studied period for each lake (10/26/2010 for Lake Morenito and 10/07/2010 for Lake Escondido). **a**–**d** Modeled spectral attenuation coefficient for the euphotic zone; **b**–**e** mean water column absorption coefficient; **c**–**f** spectral downward irradiance versus depth

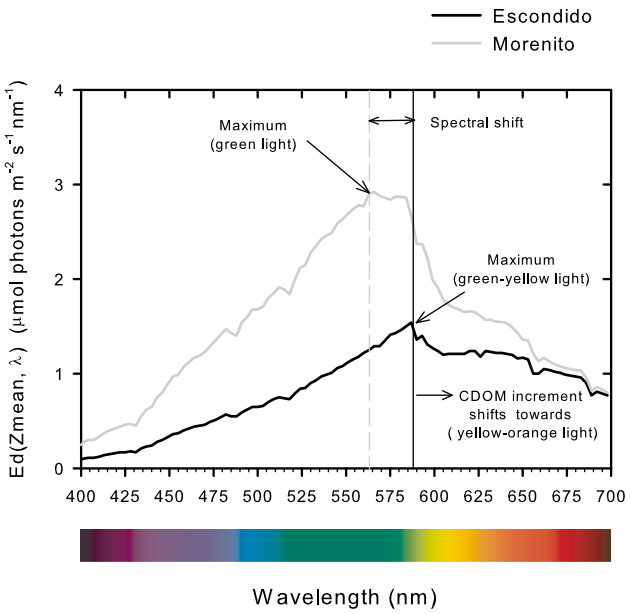

Fig. 3 Mean spectral downward irradiance in the water column of sampling dates (04/22/2010 for Lake Morenito and 09/01/2010 for Lake Escondido) showing the highest differences in the Kd(R)/Kd(G) ratio between lakes

phytoplankton abundance was similar between lakes (Table 2), but total phytoplankton biomass was slightly lower in Lake Escondido (Fig. 4a, b). The phytoplankton taxa which contributed more than 5 % of total biomass were similar in both water bodies. Autotrophs were mainly represented by the dinophyceans *Gymnodinium paradoxum* and *Peridinium* sp. in both lakes (Table 2; Fig. 4c, d). Mixotrophic algae dominated the phytoplankton community, representing more than 74 % of the total phytoplankton biomass during the year in both lakes (Fig. 4c, d). Among the mixotrophic taxa, cryptophytes were represented by *Plagioselmis lacustris* and *Cryptomonas erosa*, chrysophytes were constituted by *Dinobryon sertularia*, *D. divergens*, *Ochromonas* cf. *ovalis* and unidentified chrysophycean nanoflagellates larger than 5 µm in diameter. Moreover, dictyochophytes and haptophytes were represented by *Pseudopedinella* sp. and *Chrysochromulina parva*, respectively.

The phytoplankton community structure differed between lakes (Fig. 4c, d). The phytoplankton assemblage in Lake Escondido was dominated by chrysophytes (mean relative biomass of 34.8 %), followed by cryptophytes (mean relative biomass of 26.4 %). In contrast, the assemblage in Lake Morenito was strongly dominated by cryptophytes throughout all the study period (mean relative biomass of 61.5 %) (Fig. 4c, d). Differences in cryptophycean biomass between lakes were dependent on sampling time. Lake Morenito showed significantly higher cryptophycean biomass almost during all the studied period with exception of June, September and October (two-way RM ANOVA: $F = 5.25$, $p < 0.001$). For chrysophycean biomass, differences between lakes were also dependent on sampling time. Lake Escondido showed significantly greater chrysophycean biomass during all the studied periods except October 2010 and January 2011 (two-way RM ANOVA: $F = 8.05$, $p < 0.001$). A detailed analysis of the dominant taxa showed that cryptophycean *P. lacustris* was the most important species in Lake Morenito, while the non-loricated chrysophytes were most important in Lake Escondido.

The biomass variation of cryptophytes and chrysophytes was tightly related to Kd(R)/Kd(G) ratio. In the case of cryptophytes, this variable was the only one explaining the biomass variation according to the stepwise forward model regression, yielding: Cryptophyceae biomass $= 2.162 \times$ Kd(R)/Kd(G) ratio $+ 0.384$ (MLR: $R^2 = 0.78$, $p < 0.001$, $n = 20$). Meanwhile, in the case of chrysophytes, Kd(R)/Kd(G) ratio and temperature were included in the model significantly explained the biomass variation, yielding: Chrysophyceae biomass $= -2.334 \times$ Kd(R)/Kd(G) ratio $+ 0.962 \times$ Temperature $+ 0.323$ (MLR: $R^2 = 0.62$, $p < 0.001$, $n = 20$). As a result, the effect of the spectral composition of underwater light upon biomass was opposite for these two dominant algal groups (Fig. 5). In contrast, this pattern was not observed in the other phytoplankton groups. Similar results were obtained by considering the abiotic component of light attenuation with Cryptophyceae biomass showing a strong positive significant relationship with KdAbio(R)/KdAbio(G) ratio (LR, $R^2 = 0.81$, $p < 0.001$, $n = 20$). This was also observed for Chrysophyceae biomass showing a negative significant relationship with KdAbio(R)/KdAbio(G) ratio (LR, $R^2 = 0.52$, $p < 0.001$, $n = 20$).

Discussion

During the annual cycle, the studied lakes showed consistent differences in CDOM absorption coefficients and CDOM molecular size inferred from the spectral slope, while they did not show significant differences in a number of limnological features (i.e., temperature, dissolved oxygen, pH, and nutrient, TSS and Chl*a* concentrations). The hydrogeomorphic features of these lakes and consequently how they are related with the surrounding terrestrial ecosystem, could explain observed differences in CDOM characteristics between them. Lake Escondido showed higher $a_{CDOM}(440)$:Chl*a* ratio indicating a greater degree of allochthony than Lake Morenito. This result was likely related to the fact that Lake Escondido is a closed basin (seepage) and has a 1.35-fold higher perimeter-to-lake-area ratio than Lake Morenito. This could be associated with a higher loading rate of terrestrial carbon, explaining higher

Table 2 Summary of phytoplankton abundance (cell mL^{-1}) (mean, SD, maximum and minimum values) contributing with more than 5 % of the total phytoplankton biomass along the studied period in Lakes Escondido and Morenito

	Class	Taxa	Lake Escondido		Lake Morenito	
			Mean ± SD	Range	Mean ± SD	Range
Mixotrophic taxa	Haptophyceae	*Chrysochromulina parva*	344.4 ± 284.4	8.5 ± 1,002.8	362.3 ± 361.5	8.5 ± 1,014.7
	Cryptophyceae	*Cryptomonas erosa*	10.3 ± 6.3	1.0 ± 18.2	47.9 ± 59.9	5.0 ± 210.3
		Plagioselmis lacustris	109.4 ± 79.0	25.5 ± 290.8	404.8 ± 359.2	105.6 ± 1,251.6
	Chrysophyceae	*Ochromonas* cf. *ovalis*	500.0 ± 276.6	152.7 ± 1,008.9	210.2 ± 130.6	23.9 ± 425.6
		Chrysophyceae >5 µm	126.1 ± 76.6	0.0 ± 233.0	10.3 ± 10.9	0.0 ± 31.9
		Dinobryon divergens	20.7 ± 29.0	0.3 ± 80.7	40.4 ± 53.4	3.6 ± 184.3
		Dinobryon sertularia	7.3 ± 8.1	0.3 ± 21.1	12.0 ± 9.4	1.6 ± 29.8
	Dictyochophyceae	*Pseudopedinella* sp.	189.1 ± 64.7	99.2 ± 294.0	128.8 ± 125.7	10.3 ± 350.4
	Dinophyceae	*Gymnodinium fuscum*	0.3 ± 0.2	0.1 ± 0.9	0.6 ± 0.6	0.1 ± 1.8
		Gymnodinium varians	2.8 ± 3.0	0.2 ± 9.5	2.5 ± 1.5	0.1 ± 4.6
	Total mixotrophic		1,310.4		1,219.78	
Autotrophic taxa	Chlorophyceae	*Oocystis lacustris*	–	–	1.8 ± 0.8	1.3 ± 2.7
	Chrysophyceae	*Mallomonas* sp.	16.8 ± 13.4	7.3 ± 26.2	18.2 ± 8.78	8.8 ± 26.2
	Dinophyceae	*Gymnodinium paradoxum*	18.3 ± 20.8	5.1 ± 73.0	6.6 ± 5.9	1.0 ± 13.8
		Peridinium sp.	18.7 ± 17.3	1.4 ± 47.0	1.5 ± 0.4	1.2 ± 1.8
	Bacillariophyceae	*Synedra ulna*	2.2 ± 0.7	1.4 ± 2.8	10.8 ± 11.1	2.8 ± 23.5
		Fragilaria spp.	5.0 ± 14.6	0.1 ± 48.4	8.0 ± 14.1	0.2 ± 48.4
	Total autotrophic		61.0		46.9	

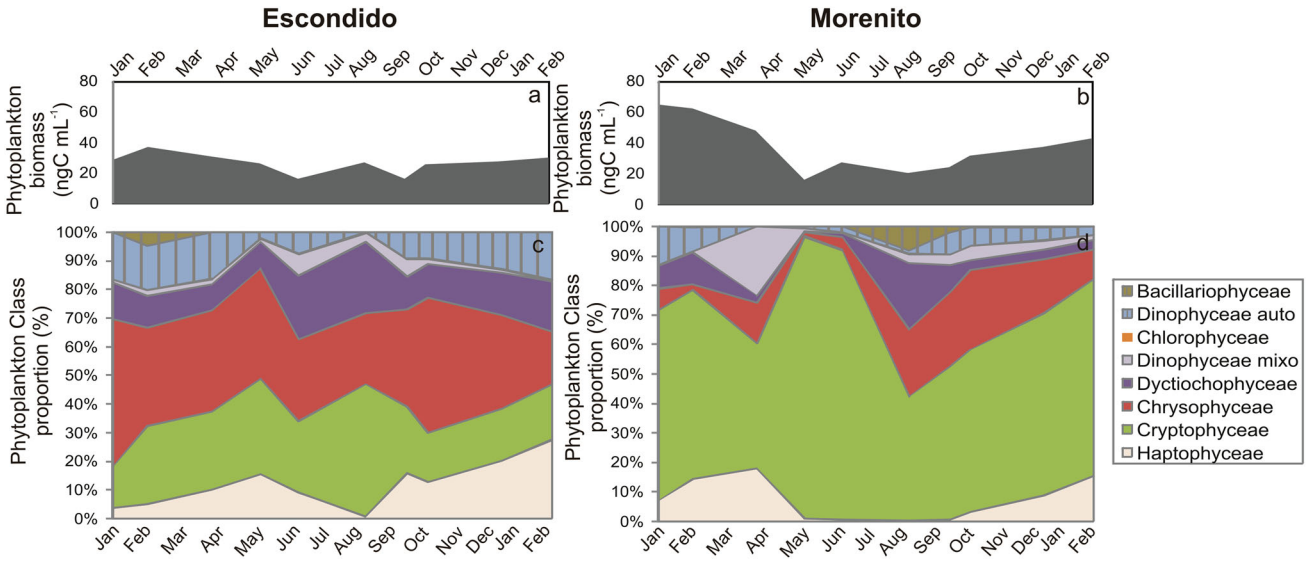

Fig. 4 **a**, **b** Temporal variation of phytoplankton biomass in Lakes Escondido and Morenito as an average of the water column values; **c**, **d** phytoplankton composition along the studied year in both lakes as an average of the water column values. *Area with vertical lines* correspond to autotrophic taxa, *area without lines* correspond to mixotrophic taxa, note that for this reason Dinophyceae was shown separately

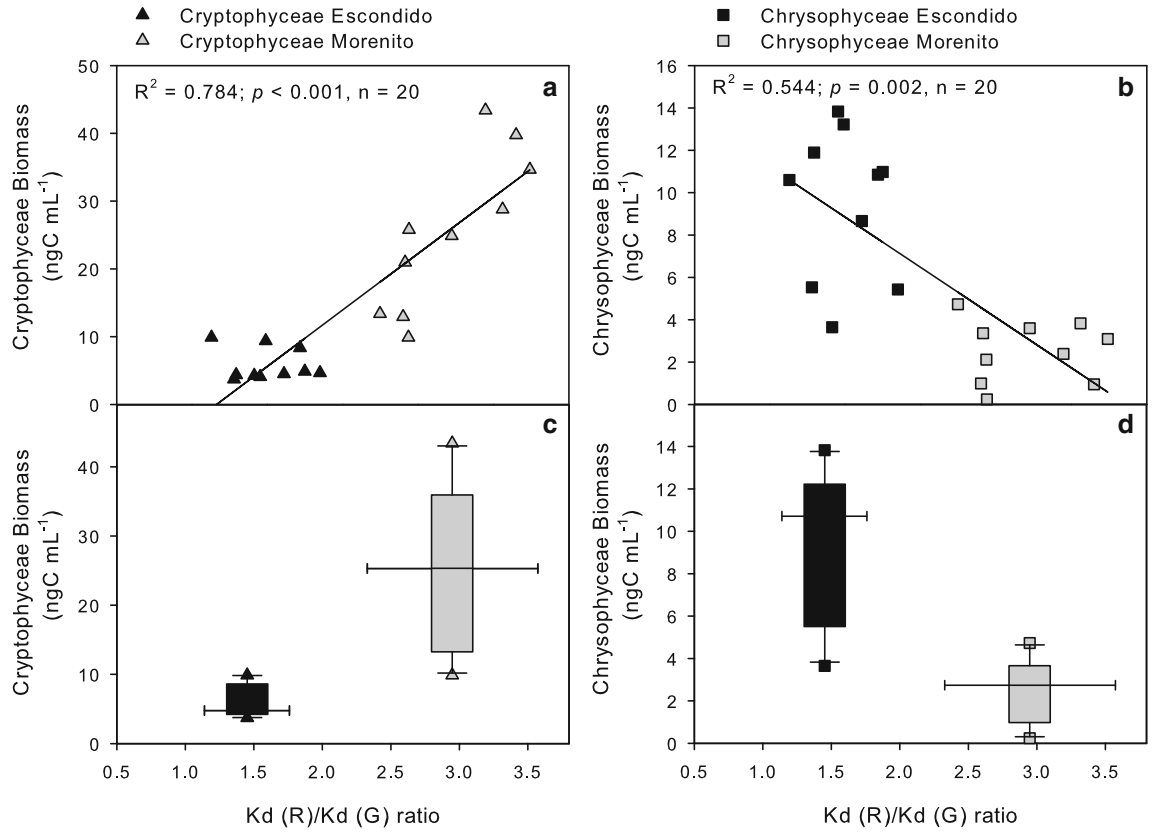

Fig. 5 Relationship between the biomass of Cryptophyceae (**a**) and Chrysophyceae (**b**) with Kd(R)/Kd(G) ratio; boxplot of Cryptophyceae (**c**) and Chrysophyceae (**d**) and Kd(R)/Kd(G) ratio relationship, *vertical bars* indicate the 75 percentile of variation of class biomass, *horizontal bars* indicate the SD of the Kd(R)/Kd(G) ratio. Note that the scale in the case of the biomass is different between the algal groups

$a_{CDOM}(440)$ and lower $S_{275–295}$ values in Lake Escondido, in accordance with similar results obtained by Webster et al. (2008) for North-temperate lakes. In spite of these differences, a synchronous variation of CDOM optical metrics was observed between lakes, probably due to the effects of external regional factors (precipitation, temperature and radiation), as was previously described in other aquatic environments (Pace and Cole 2002). Particularly, we found a good agreement between cumulative precipitation (150 days before the sampling date) and the $a_{CDOM}(440)$, which could be associated to the input of allochthonous CDOM from the watershed by leaching. Similar results relating CDOM and cumulative precipitation have been reported with a time period greater than that obtained in the present survey (Hongve et al. 2004). While some lakes with stream inflows show the effect of rainfall almost immediately, others, such as seepage lakes, do not reflect changes for months (Shaw 2004). In the case of the two studied North Patagonian lakes, which lack inflows, the period of 5 months explaining the $a_{CDOM}(440)$ variations appears to encompass the precipitation pattern characteristic of the region, with a rainy season between April and September, and a drier season between October and March. In this sense, the maximum $a_{CDOM}(440)$ values were registered towards the end of the rainy season, while the minimum values were obtained towards the end of the drier season, also due to the photobleaching processes associated to the high spring–summer radiation. These results highlight the climate driven effects on the $a_{CDOM}(440)$ dynamics of these oligotrophic shallow lakes.

Different investigations have shown that CDOM is important in determining UV and PAR transparency in lakes (Scully and Lean 1994; Morris et al. 1995; Bukaveckas and Robbins-Forbes 2000). Particularly, light attenuation in shallow Patagonian lakes could be shaped mainly by CDOM absorption (Pérez et al. 2010). Pérez et al. (2002) have described the underwater light climate of deep and shallow Patagonian lakes and its implications on Chl*a* vertical distribution. With respect to shallow lakes, including Escondido and Morenito, they found higher Kd(PAR) and Kd(GREEN) values in Lake Escondido, which in turn presented higher values of CDOM absorption coefficients. Our results support previous findings in Patagonian shallow lakes, showing that differences

between lakes in both water transparency and spectral composition of underwater light are linked to CDOM. However, regarding within-lake variation in water transparency, it is worth noting that temporal variation of Kd(PAR) in Lake Morenito was driven by CDOM and other factors. In fact, both solar angle and particulate absorption were important factors in the interpretation of water transparency in this lake. For instance, considering only solar elevation, months with highest $a_{CDOM}(440)$ values (October and November) presented higher solar altitude than June [month with highest Kd(PAR) values]. Higher solar altitude decreased light attenuation due to the diminution in the pathlength of the unscattered solar beam within the water, this effect being important in clearest waters of Lake Morenito. Regarding variation in the spectral composition of underwater light, Lake Escondido with particular CDOM spectral absorption characteristic and high $a_{CDOM}(440)$ values presented higher attenuation of blue and green light than Lake Morenito, resulting in an underwater light climate with a spectral composition shifted towards green–yellow light (570–585 nm). In contrast, in Lake Morenito wavelengths between 550 and 570 nm penetrated more deeply, resulting in an underwater light climate dominated by green light [higher Kd(R)/Kd(G) ratio and greater green light availability].

In this contribution we aimed to analyze the effect of underwater light climate on phytoplankton community structure. Light intensity and nutrient concentration, and their interaction, have been recognized as the classic "bottom-up factors". These abiotic factors regulate abundance, diversity, taxonomic composition and productivity of phytoplankton communities (Reynolds 2006). However, since the first visionary works introducing the theory known as chromatic adaptation (Engelmann 1883; Harder 1923; Dutton and Juday 1944; Glover et al. 1987), an increasing number of studies concerning competition models and laboratory experiments (Stomp et al. 2004; Sathyendranath and Platt 2007; Hickman et al. 2010) as well as field studies (Takahashi et al. 1989; Bidigare et al. 1990; Vörös et al. 1998; Stomp et al. 2007; Hickman et al. 2009; Frenette et al. 2012) have demonstrated the importance of spectral composition of underwater light as a relevant factor in modeling phytoplankton diversity and community structure. Consequently, either measurements of PAR vertical attenuation coefficients or water transparency proxies (e.g., water color, Secchi disc, nephelometric turbidity) could be insufficient to accurately describe the underwater light climate and to assess the potential importance of spectral composition of underwater light on phytoplankton selection.

As we expected from previous studies (Diaz and Pedrozo 1993; Queimaliños 2002), we found similar phytoplankton groups in both lakes, mainly belonging to phagotrophic algae. Prior work supports the idea that the mixotrophic mode of nutrition is a successful strategy under nutrient limiting conditions (e.g., Nygaard and Tobiesen 1993; Katechakis and Stibor 2006; Unrein et al. 2007). The low nutrient concentrations measured in the present study were similar to those found previously (Diaz and Pedrozo 1993; Queimaliños 2002), reinforcing the fact that nutrient limiting conditions exist in these oligotrophic North Patagonian lakes (Diaz et al. 2007). This fact would partially explain the success of mixotrophic algae over autotrophic ones in these environments. However, despite the remarkable similarity in nutrient concentration and phytoplankton species composition between lakes, a clear difference was observed in the relative abundance of each taxon in each lake (Fig. 4). Such results are likely not explained solely by nutrient limitation, but may be associated with differences in the spectral composition of the underwater light of these lakes. In the present study we followed the approach of Pick (1991) and Vörös et al. (1998), analyzing the spectral composition of the underwater light and its relationship with the phytoplankton community structure. Field data showed a striking relationship between the Kd(R)/Kd(G) ratio and the biomass of the two dominant phytoplankton classes (Cryptophyceae and Chrysophyceae) (Figs. 5, 6). Interestingly, we found that Kd(PAR) values, $a_{CDOM}(440)$ values, as well as mean daily PAR irradiance of the water column were not included in the MLR models assessed for explaining differences in dominant phytoplankton classes. This implies that each one of these variables did not explain or explained lower variation than that explained by Kd(R)/Kd(G) ratio. The fact that CDOM has a dominant effect driving differences in spectral composition of underwater light either between lakes or in the within-lake variation was key in the mechanistic reasoning utilized here. Indeed, similar results were obtained if the analysis of the effects of underwater light climate on phytoplankton composition was restricted to the abiotic component of light attenuation (i.e., absorption by CDOM, water itself and solar elevation) (data not shown). Phytoplankton absorption did not contribute significantly in the light spectral composition that shapes its own habitat in these lakes.

Our results complement the investigations of Vörös et al. (1998) and Stomp et al. (2007), which showed that the distribution patterns of picocyanobacteria types on natural waters are strongly related to the underwater light spectra. Differences in picocyanobacteria accessory pigmentation (mainly phycobiliproteins), and therefore distinctive selective absorption bands, allow better alternative exploitation of green or red light with direct implications on their growth rates. The result of this is a gradual transition from predominance of PE-rich cells in clear waters (green and blue were the most penetrating lights) to PC-

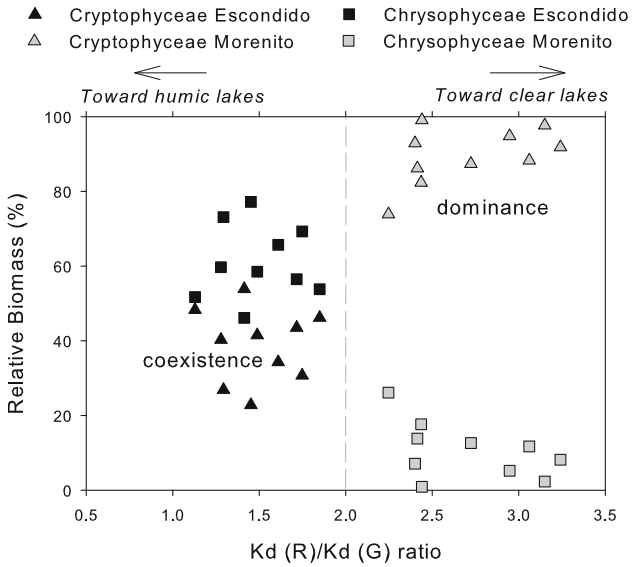

Fig. 6 Relative biomass of Cryptophyceae and Chrysophyceae respect to the sum of these two groups in response to the Kd(R)/Kd(G) ratio

rich cells in turbid ones (red light penetrated farthest) (Vörös et al. 1998). This environmental selection (or niche differentiation) of algae with pigment absorption bands matching the prevailing spectral composition of underwater light, might also be applied to the observed biomass pattern of cryptophytes in Escondido and Morenito. Cryptophytes are the sole organisms that have the unique pigment combination of Chl*a*, Chl*c*2, and the carotenoid alloxanthin in addition to one of the two phycobiliproteins, PE or PC (Hill and Rowan 1989; Doust et al. 2006). In particular, species of *Cryptomonas* spp. and *Plagioselmis* spp. (syn. *Rhodomonas*) have been previously reported to possess the biliprotein PE (Beutler et al. 2002; Dinshaw 2012), and specifically, *P. lacustris* bears PE with a maximum absorbance at 550 nm (Hill and Rowan 1989). In that sense, this PE absorption maximum would favor light harvesting in Lake Morenito characterized by a relatively greater availability of green light than Lake Escondido, explaining the observed higher biomass of cryptophytes in the former. Furthermore, on the assumption that the gradient of light conditions experienced by phytoplankton cells in a mixed water column could be represented by the mean spectral downward light component of pelagic zone, in Lake Escondido the underwater light is shifted towards green–yellow wavelengths with a maximum value around 585 nm (Fig. 3). This scenario allows the coexistence of Cryptophyceae and Chrysophyceae algae, but it does not favor the dominance of PE containing cryptophytes. These results are coincident with those observed by Stomp et al. (2007, see their Fig. 1a) in the scenario II of model simulations. In this modeled optical scenario, spectral irradiance is neither dominated by green nor red light, allowing the coexistence of Red and Green picocyanobacteria types. In general, our outcomes suggest that a ratio of Kd(R)/Kd(G) below 2 appears to be a limit for the dominance of cryptophytes, meanwhile a ratio >2 allows them to comparatively thrive (Figs. 5c, d, 6).

Of course, competition for light is not the whole story. Even if light (intensity and spectral composition) could play a central role in structuring the habitat, it represents just one of several factors that shape the niches of different phytoplankton species. Other factors like predation could also shape, in some degree, phytoplankton assemblages. Concurrent zooplankton sampling (data not shown) revealed that Lake Morenito had a higher zooplanktonic biomass with a higher proportion of cladocerans compared to Lake Escondido, which is dominated by rotifers. These differences could be explained by the prevailing cryptophytes in Lake Morenito, since they constitute a high quality food for the cladocerans due to the presence of polyunsaturated fatty acids which favor the growth and reproduction of these zooplankters (Burns et al. 2011). However, it would not explain the dominant biomass pattern observed between lakes.

Overall, the novelty of our study relies on how precipitation/hydrological patterns may induce shifts in the dominant phytoplankton species through CDOM dynamics. Moreover, we present field evidence showing the link between CDOM and spectral composition of underwater light, and its effects on nano- and microphytoplankton community structure (differences in Cryptophyceae and Chrysophyceae biomass) of two natural freshwater systems. Like other evidence in marine and freshwater systems the present investigation showed that species selection in the spectral composition of underwater light environment could play an important role determining phytoplankton community structure (Stomp et al. 2004, 2007; Callieri 2007; this study) and ultimately primary productivity. In line with this, very recent studies developed in boreal lakes demonstrated the negative effect of CDOM on primary productivity through shading effect (Thrane et al. 2014; Seekell et al. 2015).

Finally, considering that global climate change may alter mean temperature, precipitation patterns, cloud cover and wind speed, it could also modify the underwater light climate in lakes. In particular, climate change predictions for the North Patagonian region indicate a reduction of winter precipitation (Villalba et al. 2012) and an increase in summer (Núñez et al. 2009). In this region, an increase in precipitation could produce an increase in CDOM inputs to lakes during the main photobleaching period (summer) and a reduction during the winter season. Consequently, transparency and the green light availability would increase in these lakes. Based on these predictions, it is possible that

the phytoplankton composition of our lakes could change towards the dominance of Cryptophyceae, even in the more humic Lake Escondido. However, it is important to consider that in many other environments around the world the opposite pattern is occurring; in fact, there is a strong increase of terrestrial DOM concentration in surface waters in the Arctic, due to the permafrost thawing (Guo et al. 2007; Fichot et al. 2013), as well as with the increment of precipitation favoring runoff (Pace and Cole 2002; Hongve et al. 2004; Zepp et al. 2011). Thus, alternative changes in the rates of input of CDOM would alter the underwater light climate in a water body and, consequently, a change in the natural productivity of the environment would occur.

Acknowledgments We are very grateful to Dr. Stefan Simis, Dr. Jean-François Lapierre and one anonymous reviewer, whose valuable contributions were essential to improve the manuscript. We especially thank Miguel, Nicolás and Leandro Battini, Dr. Cristian D. Torres, and Nelson Del Moral for their help during the sampling. This work was supported by the Consejo Superior de Investigaciones Científicas-Consejo Nacional de Investigaciones Científicas y Técnicas (CSIC-CONICET) (Spain-Argentina) Project PROBA (2007 AR0018, CSIC) and the Argentinean projects CONICET-PIP 01301, FONCYT-PICT 2007-00393 and PICT 2012-1200, and UNComahue 04/B166 and 04/B194. Marina Gerea and Carolina Soto Cárdenas were supported by CONICET fellowships. Gonzalo L. Pérez, Fernando Unrein and Claudia Queimaliños are CONICET researchers (Argentina). Donald Morris is a researcher and faculty member at Lehigh University (United States).

References

AIC (2011) Informe Hidrometeorológico 2010–2011. Autoridad Interjurisdiccional de Cuencas, Río Negro

Alonso C, Rocco V, Barriga JP, Battini MA, Zagarese H (2004) Surface avoidance by freshwater zooplankton: field evidence on the role of ultraviolet radiation. Limnol Oceanogr 49:225–232

APHA (2005) Standard methods for the examination of water and wastewater. American Public Health Association, Washington

Asmala E, Stedmon CA, Thomas DN (2012) Linking CDOM spectral absorption to dissolved organic carbon concentrations and loadings in boreal estuaries. Estuar Coast Shelf Sci 111:107–117

Bachmann RW, Canfield DE (1996) Use of an alternative method for monitoring total nitrogen concentration in Florida lakes. Hydrobiologia 323:1–8

Balseiro EG, Modenutti B (1990) Zooplankton dynamics of Lake Escondido (Río Negro, Argentina), with special reference to a population of *Boeckella gracilipes* (Copepoda, Calanoida). Int Rev Hydrobiol 75:475–491

Bastidas Navarro M, Modenutti B, Callieri C, Bertoni R, Balseiro E (2009) Balance between primary and bacterial production in North Patagonian shallow lakes. Aquat Ecol 43:867–878

Belzile C, Vincent WF, Kumagai M (2002) Contribution of absorption and scattering to the attenuation of UV and photosynthetically available radiation in Lake Biwa. Limnol Oceanogr 47:95–107

Beutler M, Wiltshire KH, Meyer B et al (2002) A fluorometric method for the differentiation of algal populations in vivo and in situ. Photosynth Res 72:39–53

Bidigare R, Marra J, Dickey T, Iturriaga R, Baker K, Smith R, Pak H (1990) Evidence for phytoplankton succession and chromatic adaptation in the Sargasso Sea during spring 1985. Mar Ecol Prog Ser 60:113–122

Bukaveckas PA, Robbins-Forbes M (2000) Role of dissolved organic carbon in the attenuation of photosynthetically active and ultraviolet radiation in Adirondack lakes. Freshw Biol 43:339–354

Burns CW, Brett MT, Schallenberg M (2011) A comparison of the trophic transfer of fatty acids in freshwater plankton by cladocerans and calanoid copepods. Freshw Biol 56:889–903

Callieri C (2007) Picophytoplankton in freshwater ecosystems: the importance of small-sized phototrophs. Freshw Rev 1:1–28

Carpenter SR, Cole JJ, Kitchell JF, Pace ML (1998) Impact of dissolved organic carbon, phosphorus, and grazing on phytoplankton biomass and production in experimental lakes. Limnol Oceanogr 43:73–80

Diaz M, Pedrozo F (1993) Seasonal succession of phytoplankton in a small Andean Patagonian lake (Rep. Argentina) and some considerations about the PEG model. Arch Hydrobiol 127:167–184

Diaz M, Pedrozo F, Reynolds C, Temporetti P (2007) Chemical composition and the nitrogen-regulated trophic state of Patagonian lakes. Limnologica 37:17–27

Dinshaw R (2012) Spectroscopic investigations of the photophysics of cryptophyte light-harvesting. University of Toronto, Canada

Doust AB, Wilk KE, Curmi PMG, Scholes GD (2006) The photophysics of cryptophyte light-harvesting. J Photochem Photobiol Chem 184:1–17

Dutton HJ, Juday C (1944) Chromatic adaptation in relation to color and depth distribution of freshwater phytoplankton and large aquatic plants. Ecology 25:273–282

Engelmann TW (1883) *Bacterium photometricum*: ein Beitrag zur vergleichenden Physiologie des Licht- und Farbensinnes. Arch Physiol 30:95–124

Falkowski PG, Katz ME, Knoll AH, Quigg A, Raven JA, Schofield O et al (2004) The evolution of modern eukaryotic phytoplankton. Science 305:354–360

Ferrero E, Eöry M, Ferreyra G et al (2006) Vertical mixing and ecological effects of ultraviolet radiation in planktonic communities. Photochem Photobiol 82:898–902

Fichot CG, Kaiser K, Hooker SB, Amon RMW, Babin M, Bélanger S, Walker SA, Benner R (2013) Pan-Arctic distributions of continental runoff in the Arctic Ocean. Sci Rep 3:1053

Frenette JJ, Massicotte P, Lapierre JF (2012) Colorful niches of phytoplankton shaped by the spatial connectivity in a large river ecosystem: a riverscape perspective. PLoS One 7:e35891

Gallegos CL (1994) Refining habitat requirements of submersed aquatic vegetation: role of optical models. Estuaries 17:187–199

Gallegos CL (2001) Calculating optical water quality targets to restore and protect submersed aquatic vegetation: overcoming problems in partitioning the diffuse attenuation coefficient for photosynthetically active radiation. Estuaries 24:381–397

Gause GF (1934) The struggle for existence. William and Wilkins, Baltimore

Glover HE, Keller MD, Spinrad RW (1987) The effects of light quality and intensity on photosynthesis and growth of marine eukaryotic and prokaryotic phytoplankton clones. J Exp Mar Biol Ecol 105:137–159

Green SA, Blough NV (1994) Optical absorption and fluorescence properties of chromophoric dissolved organic matter in natural waters. Limnol Oceanogr 39:1903–1916

Guo L, Ping C-L, Macdonald RW (2007) Mobilization pathways of organic carbon from permafrost to arctic rivers in a changing climate. Geophys Res Lett 34:L13603

Häder DP, Kumar HD, Smith RC, Worrest RC (2007) Effects of solar UV radiation on aquatic ecosystems and interactions with climate change. Photochem Photobiol Sci 6:267–285

Harder R (1923) Über die Bedeutung von Lichtintensitt und Wellenlänge für die Assimilation farbiger Algen. Z Bot 15:306–355

Helms JR, Stubbins A, Ritchie JD, Minor EC, Kieber DJ, Mopper K (2008) Absorption spectral slopes and slope ratios as indicators of molecular weight, source, and photobleaching of chromophoric dissolved organic matter. Limnol Oceanogr 53:955–969

Hickman AE, Holligan PM, Moore CM, Sharples J, Krivtsov V, Palmer MR (2009) Distribution and chromatic adaptation of phytoplankton within a shelf sea thermocline. Limnol Oceanogr 54:525–536

Hickman A, Dutkiewicz S, Williams R, Follows M (2010) Modelling the effects of chromatic adaptation on phytoplankton community structure in the oligotrophic ocean. Mar Ecol Prog Ser 406:1–17

Hill DRA, Rowan KS (1989) The biliproteins of the Cryptophyceae. Phycologia 28:455–463

Hiriart-Baer V (2013) Dissolved organic matter quantity and quality in Lake Simcoe compared to two other large lakes in southern Ontario. Inland Waters 3:139–152

Hongve D, Riise G, Kristiansen JF (2004) Increased colour and organic acid concentrations in Norwegian forest lakes and drinking water—a result of increased precipitation? Aquat Sci 66:231–238

Huang W, Chen RF (2009) Sources and transformations of chromophoric dissolved organic matter in the Neponset River Watershed. J Geophys Res 114:G00F05–G00F19

Jobbágy EG, Paruelo JM, León RJC (1995) Estimación del régimen de precipitación a partir de la distancia a la cordillera en el noroeste de la Patagonia, Argentina. Ecología Austral 5:47–53

Jones RI (1992) The influence of humic substances on lacustrine planktonic food chains. Hydrobiologia 229:73–91

Jones RI (1994) Mixotrophy in planktonic protist as a spectrum of nutritional strategies. Mar Microb Food Webs 8(1–2):87–96

Karlsson J, Byström P, Ask J et al (2009) Light limitation of nutrient-poor lake ecosystems. Nature 460:506–509

Katechakis A, Stibor H (2006) The mixotroph *Ochromonas tuberculata* may invade and suppress specialist phago- and phototroph plankton communities depending on nutrient conditions. Oecologia 148:692–701

Kirk J (1981) Monte Carlo study of the nature of the underwater light field in, and the relationships between optical properties of, turbid yellow waters. Aust J Mar Freshw Res 32:517–532

Kirk J (1984) Dependence of relationship between inherent and apparent optical properties of water on solar altitude. Limnol Oceanogr 29:350–356

Kirk J (1991) Volume scattering function, average cosines, and the underwater light field. Limnol Oceanogr 36:455–467

Kirk J (1994) Characteristics of the light field in highly turbid waters: a Monte Carlo study. Limnol Oceanogr 39:702–706

Kirk J (2011) Light and photosynthesis in aquatic ecosystems. Cambridge University Press, New York

Lawrenz E, Pinckney JL, Ranhofer ML et al (2010) Spectral irradiance and phytoplankton community composition in a Blackwater-dominated estuary, Winyah Bay, South Carolina, USA. Estuar Coast 33:1186–1201

Leavitt PR, Vinebrooke RD, Donald DB, Smol JP, Schindler DW (1997) Past ultraviolet radiation environments in lakes derived from fossil pigments. Nature 388:457–459

Menden-Deuer S, Lessard EJ (2000) Carbon to volume relationships for dinoflagellates, diatoms, and other protist plankton. Limnol Oceanogr 45:569–579

Mladenov N, Sommaruga R, Morales-Baquero R et al (2011) Dust inputs and bacteria influence dissolved organic matter in clear alpine lakes. Nat Commun 2:405

Modenutti BE, Balseiro EG, Queimalinos CP (2000) Ciliate community structure in two South Andean lakes: the effect of lake water on *Ophrydium naumanni* distribution. Aquat Microb Ecol 21:299–307

Morel A, Gentili B (1991) Diffuse reflectance of oceanic waters: its dependence on sun angle as influenced by the molecular scattering contribution. Appl Opt 30:4427–4438

Morris DP, Zagarese H, Williamson CE, Balseiro EG et al (1995) The attenuation of solar UV radiation in lakes and the role of dissolved organic carbon. Limnol Oceanogr 40:1381–1391

Nayar S, Chou LM (2003) Relative efficiencies of different filters in retaining phytoplankton for pigment and productivity studies. Estuar Coast Shelf Sci 58:241–248

Núñez MN, Solman SA, Cabré MF (2009) Regional climate change experiments over southern South America. II: climate change scenarios in the late twenty-first century. Clim Dyn 32:1081–1095

Nusch EA (1980) Comparison of different methods for chlorophyll and phaeopigment determination. Arch Hydrobiol 14:14–36

Nygaard K, Tobiesen A (1993) Bacterivory in algae: a survival strategy during nutrient limitation. Limnol Oceanogr 38:273–279

Pace ML, Cole JJ (2002) Synchronous variation of dissolved organic carbon and color in lakes. Limnol Oceanogr 47:333–342

Palenik B (2001) Chromatic adaptation in marine *Synechococcus* strains. Appl Environ Microbiol 67:991–994

Paruelo JM, Beltrán A, Jobbágy E et al (1998) The climate of Patagonia: general patterns and controls on biotic processes. Ecol Austral 8:85–101

Pérez GL (2006) Light climate and pigment distribution in Andean Patagonian Lakes. PhD thesis, Universidad Nacional del Comahue, Argentina

Pérez GL, Queimaliños C, Modenutti BE (2002) Light climate and plankton in the deep chlorophyll maxima in North Patagonian Andean lakes. J Plankton Res 24:591–599

Pérez GL, Torremorell A, Bustingorry J et al (2010) Optical characteristics of shallow lakes from the Pampa and Patagonia regions of Argentina. Limnologica 40:30–39

Pick FR (1991) The abundance and composition in relation to light penetration of freshwater picocyanobacteria. Limnol Oceanogr 36:1457–1462

Pienitz R, Vincent WF (2000) Effect of climate change relative to ozone depletion in subarctic lakes. Nature 404:484–487

Pope RM, Fry ES (1997) Absorption spectrum (380–700 nm) of pure water. II. Integrating cavity measurements. Appl Opt 36:8710–8723

Porter KG, Feig Y (1980) The use of DAPI for identifying aquatic microflora. Limnol Oceanogr 25:943–948

Queimaliños C (1993) Efectos del zooplancton sobre la dinámica sucesional del fitoplancton en un ambiente lacustre andino. PhD thesis, Universidad de Buenos Aires, Argentina

Queimaliños C (2002) The role of phytoplanktonic size fractions in the microbial food webs in two north Patagonian lakes (Argentina). Arch Hydrobiol 28:1236–1240

Queimaliños C, Reissig M, Diéguez MDC et al (2012) Influence of precipitation, landscape and hydrogeomorphic lake features on pelagic allochthonous indicators in two connected ultraoligotrophic lakes of North Patagonia. Sci Tot Environ 427–428:219–228

Quirós R, Drago E (1999) The environmental state of Argentinean lakes: an overview. Lakes Reserv Res Manag 4:55–64

Rapacioli (2011) Caracterización hidrológica de la reserva natural urbana Lago Morenito-Laguna Ezquerra. In: Abalerón A, Proyecto de Manejo de Reserva Natural Morenito-Ezquerra. Fundación Bariloche

Reynolds CS (2006) Ecology of phytoplankton. Cambridge University Press, Cambridge

Sanders RW, Porter KG (1988) Phagotrophic phytoflagellates. Adv Microb Ecol 10:167–192
Sathyendranath S, Platt T (2007) Spectral effects in bio-optical control on the ocean system. Oceanologia 49:5–39
Schindler DW, Curtis PJ, Bayley SE, Parker BR, Beaty KG, Stainton MP (1997) Climate-induced changes in the dissolved organic carbon budgets of boreal lakes. Biogeochemistry 36:9–28
Scully NM, Lean DRS (1994) The attenuation of ultraviolet light in temperate lakes. Ergeb Limnol 43:135–144
Seekell DA, Lapierre J-F, Ask J, Bergström A-K, Deininger A, Rodríguez P, Karlsson J (2015) The influence of dissolved organic carbon on primary production in northern lakes. Limnol Oceanogr 60:1276–1285
Shaw B (2004) Understanding lake data. Univ Wisconsin Pub, USA
Smith RC, Baker KS (1981) Optical properties of the clearest natural waters (200–800 nm). Appl Opt 20:177–184
Stomp M, Huisman J, De Jongh F et al (2004) Adaptive divergence in pigment composition promotes phytoplankton biodiversity. Nature 432:104–107
Stomp M, Huisman J, Vörös L et al (2007) Colourful coexistence of red and green picocyanobacteria in lakes and seas. Ecol Lett 10:290–298
Sun J, Liu D (2003) Geometric models for calculating cell biovolume and surface area for phytoplankton. J Plankton Res 25:1331–1346
Takahashi M, Ichimura S, Kishino M, Okami N (1989) Shade and chromatic adaptation of phytoplankton photo-synthesis in a thermally stratified sea. Mar Biol 100:401–409
Thrane J-E, Hessen DO, Andersen T (2014) The absorption of light in lakes: negative impact of dissolved organic carbon on primary productivity. Ecosystems 17:1040–1052
Tranvik LJ, Porter KG, Sieburth JM (1989) Occurrence of bacterivory in *Cryptomonas*, a common freshwater phytoplankter. Oecologia 78:473–476
Unrein F, Massana R, Alonso-Sáez L, Gasol JM (2007) Significant year-round effect of small mixotrophic flagellates on bacterioplankton in an oligotrophic coastal system. Limnol Oceanogr 52:456–469
Villalba R, Lara A, Masiokas MH et al (2012) Unusual Southern Hemisphere tree growth patterns induced by changes in the Southern annular mode. Nat Geosci 5:793–798
Vincent WF, Laurion I, Pienitz R (1998) Arctic and Antarctic lakes as optical indicators of global change. Ann Glaciol 27:691–696
Vörös L, Callieri C, Balogh K, Bertoni R (1998) Freshwater picocyanobacteria along a trophic gradient and light quality range. Hydrobiologia 369(370):117–125
Walsh JJ et al (2003) Phytoplankton response to intrusions of slope water on the West Florida Shelf: models and observations. J Geophys Res Oceans 108:21–31
Webster KE, Soranno PA, Cheruvelil KS et al (2008) An empirical evaluation of the nutrient-color paradigm for lakes. Limnol Oceanogr 53:1137–1148
Wood AM (1985) Adaptation of photosynthetic apparatus of marine ultraphytoplankton to natural light fields. Nature 316:253–255
Wood AM, Phinney DA, Yentsch CS (1998) Water column transparency and the distribution of spectrally distinct forms of phycoerythrin-containing organisms. Mar Ecol Prog Ser 162:25–31
Zepp RG, Erickson DJ III, Paul ND, Sulzberger B (2011) Effects of solar UV radiation and climate change on biogeochemical cycling: interactions and feedbacks. Photochem Photobiol Sci 10:261–279